incident on the cylindrical surface reduces, because more of the radiation is incident on the end-plugged annular disks. But if r_t is reduced at a fixed r_s, the percentages of radiation incident on the cylindrical surface and on the end-plugged annular disks increase, due to reduction of the obstruction. Hence, from Fig. 4a, $F_{si1-si2}$ is seen to go through an optimum with respect to r_s/r_t, for small values of d, whereas for larger values of d, it monotonically increases. This optimum is not observed in Fig. 4b. When r_t is fixed as in Fig. 4a and $(r_s/r_t) \to \infty$, $r_s \to \infty$, the shell reduces to a flat plate, and the surfaces $si1$ and $si2$ reduce to strips on the flat plate, for which $F_{si1-si2} = 0$ for any value of $(L_1 + d)$. However, when r_s is fixed as in Fig. 4b and $(r_s/r_t) \to \infty$, $r_t \to 0$ and $F_{si1-si2}$ reduces to the view factor between coaxial cylinders of equal radius without obstruction, derived analytically by Leuenberger and Person.[4] (This view factor is indicated by the dashed curve in Fig. 4b.) When r_s is fixed and $(r_s/r_t) \to 1$, the tube completely obstructs the radiation emitted by the shell, and $F_{si1-si2} = 0$. When both r_s and r_t are not fixed and both $(r_s, r_t) \to \infty$, $(r_s/r_t) \to 1$, and the two cylinders reduce to two flat plates, and again, $F_{si1-si2} = 0$. Also, when both $(r_s, r_t) \to 0$, $(r_s/r_t) \to 1$, and again, $F_{si1-si2} = 0$, because the inner tube completely obstructs the radiation. Hence, when the view factors are plotted for various r_s/r_t, the radius that is fixed must be specified.

The role of the tube in the view factor $F_{si1-si2}$ is limited to the radiation obstructed by it and not the reflected radiation. The reflected radiation is catered by the irradiation from the tube, and the amount incident on the shell surface is dictated by the view factor between tube exterior and shell interior surface elements, discussed by Tso and Mahulikar.[9]

Conclusion

The view factors for the three cases of shell interior surface segments are obtained analytically [Eqs. (4), (7), and (9)], and the analytical results agree well with the available reported numerical results. The results for the three cases can also be expressed by a single equation [Eq. (10)]. The analytical solutions are used to generate view factors for various radius ratios, which provide an insight into the complex nature of this view factor. The results generated for different radius ratios, keeping the tube and shell radius fixed separately, indicate differences, which implies that the radius that is fixed must also be specified.

Acknowledgment

The authors gratefully acknowledge the support provided by the National Science and Technology Board of Singapore, Project Number JTARC 5/96.

References

[1]Siegel, R., and Howell, J. R., *Thermal Radiation Heat Transfer*, McGraw–Hill, New York, 1992, pp. 980–1037.

[2]Brockmann, H., "Improved Treatment of Two-Dimensional Neutral Particle Transport Through Voids Within the Discrete Ordinates Method by Use of Generalized View Factors," *Deterministic Methods in Radiation Transport*, edited by A. F. Rice and R. W. Roussin, Oak Ridge National Lab., Oak Ridge, TN, 1992.

[3]Emery, A. F., Johansson, O., Lobo, M., and Abrous, A., "A Comparative Study of Methods for Computing the Diffuse Radiation Viewfactors for Complex Structures," *Journal of Heat Transfer*, Vol. 113, No. 2, 1991, pp. 413–422.

[4]Leuenberger, H., and Person, R. A., "Compilation of Radiation Shape Factors for Cylindrical Assemblies," American Society of Mechanical Engineers, Paper 56-A-144, 1956.

[5]Reid, R. L., and Tennant, J. S., "Annular Ring View Factors," *AIAA Journal*, Vol. 11, No. 10, 1973, pp. 1446–1448.

[6]Rea, S. N., "Rapid Method for Determining Concentric Cylinder Radiation View Factors," *AIAA Journal*, Vol. 13, No. 8, 1975, pp. 1122, 1123.

[7]Howell, J. R., *A Catalog of Radiation Configuration Factors*, McGraw–Hill, New York, 1982, pp. 89–220.

[8]Brockmann, H., "Analytic Angle Factors for the Radiant Interchange Among the Surface Elements of Two Concentric Cylinders," *International Journal of Heat and Mass Transfer*, Vol. 37, No. 7, 1994, pp. 1095–1100.

[9]Tso, C. P., and Mahulikar, S. P., "View Factor for Ring Elements on Coaxial Cylinders," *Journal of Thermophysics and Heat Transfer*, Vol. 13, No. 1, 1999, pp. 155–158.

Shock/Viscous Interaction Effects on Nonequilibrium-Dissociated Heating Along Arbitrarily Catalytic Surfaces

George R. Inger*
Iowa State University, Ames, Iowa 50011-3231

Nomenclature

C	$= \mu T_\infty/\mu_\infty T$, Chapman–Rubesin parameter
C_f	$= 2\upsilon_w/\rho_\infty U_\infty^2$, skin friction coefficient
C_p	= specific heat of the mixture
g	= net gas-phase reaction function (see Appendix)
H	= partial total enthalpy, $C_pT + u^2/2$
h_D	= dissociation energy per unit mass
$\hat{h}_D$	$= \beta^{1/4} h_D/P_R^{1/3}(H_{\mathrm{ADIAB}} - H_w) C_{\mathrm{REF}}^{1/8} \lambda^{3/4} (T_w/T_\infty)^{1/2}$
I_R	= reaction rate integral (see Appendix)
K_H	$= (\gamma+1)\lambda^{1/2} M_\infty^2 C_{\mathrm{REF}}{}^{1/4} \varepsilon^2/4\beta^{1/2}$
K_w	= catalytic wall recombination velocity
L	= reference length (see Fig. 1)
M	= Mach number
P_R	= Prandtl number
p	= static pressure
q_D	= diffusive heat transfer; Eq. (24)
q_w	= wall heat transfer rate
R_u, R_m	= universal and molecular gas constants, respectively
Re_L	$= \rho_\infty U_\infty L/\mu_\infty$, Reynolds number $\equiv \varepsilon^{-8}$
S_c	= Schmidt number
s_e	= total streamline slope along the boundary-layer edge; Eq. (18)
T	= absolute static temperature
$\hat{T}$	$= \beta^{1/4}(T - T_w)/P_R^{1/3}(T_{\mathrm{ADIAB}} - T_w)\varepsilon P_R^{1/3} C_{\mathrm{REF}}^{1/8} \lambda^{3/4} (T_w/T_\infty)^{1/2}$
T_t	$= Ho_\infty/Cp$, freestream total temperature
U_∞	= freestream velocity at edge of incoming boundary layer
u, v	= velocity components in x, y directions, respectively
x, y	= streamwise and normal coordinates, respectively
α	= atom mass fraction
β	$= (M_\infty^2 - 1)^{1/2}$
Γ_c	= catalytic surface Damköhler number (see Appendix)
Γ_G, $\hat{\Gamma}_G$	= gas-phase Damköhler numbers (see Appendix)
$\tilde{\Gamma}_{i_w}$	$= C_{\mathrm{REF}}^{1/8} \lambda^{1/4} (T_w/T_\infty)^{1/2} S_c^{1/3} \alpha_{e_0} \Gamma_{c0}/\beta^{1/4}(1 + \Gamma_{c0})$
γ	= specific heat ratio for frozen flow
δ^*	= displacement thickness variable
Θ	= flow deflection angle
λ	= 0.332 (Blasius solution constant)
λ_T	$= P_R^{1/3}(T_{\mathrm{ADIAB}} - T_w)(1 + \Gamma_{c0})/S_c^{1/3} \alpha_{e_0}(1 - \Gamma_G I_R)\Gamma_{c0}$
μ	= coefficient of viscosity
ρ	= density
υ_w	= wall shear stress
ω	= viscosity temperature-dependence exponent ($\mu \sim T^\omega$)

Subscripts

ADIAB	= adiabatic wall conditions
B	= body surface
e	= local inviscid flow conditions at boundary-layer edge
i.s.	= incipient separation
REF	= based on reference temperature

Received 21 May 1998; presented as Paper 98-2814 at the AIAA 29th Fluid Dynamics Conference, Albuquerque, NM, 15–18 June 1998; revision received 26 February 1999; accepted for publication 2 March 1999.

*Professor, Department of Aerospace Engineering and Engineering Mechanics. Associate Fellow AIAA.

w = wall surface conditions
0 = undisturbed boundary layer ahead of interaction zone
∞ = freestream conditions

Superscript

$(\hat{\ })$ = nondimensional variables from triple-deck theory; Eqs. (4–13)

I. Introduction

INTERACTIONS between oblique shock waves and boundary layers must be understood to predict the performance of aerodynamic devices such as flaps, spoilers, and inlets. These involve a strong viscous–inviscid interaction flow with a large local adverse pressure gradient that often provokes boundary-layer separation. A knowledge of the corresponding heat transfer disturbances in such interaction zones is also of interest because of their importance in the aerothermodynamic design of cooled hypersonic flight vehicles and because such heat transfer is itself an important diagnostic in understanding the interactive flow and its separation.

The slight influence of dissociation and surface catalysis on pressure and skin friction within a laminar boundary-layer/shock interaction has been studied numerically.[1] However, the reverse problem of how shock interaction affects the heat transfer in such nonequilibrium-dissociated flows is more interesting. Because this problem arises for either impinging shocks within hypersonic inlets or control surface-generated shocks on aerodynamic vehicles, it is addressed here from a fundamental analytical rather than numerical viewpoint. The approach used is a first-order asymptotic analysis based on a triple-deck model, generalized to include a nonequilibrium-dissociated gas phase and an arbitrary degree of surface atom catalysis at nonadiabatic wall temperatures.

II. Formulation of the Analysis

We consider a two-dimensional steady laminar flow of a binary atom–molecule dissociated gas mixture with equal specific heats in the local interaction region associated with a compression corner (Fig. 1); the companion impinging shock problem follows similar lines.[2] Large-scale global viscous–inviscid interaction effects or upstream nose bluntness effects are neglected. The disturbance-flow physics within such a short-ranged viscous–inviscid interaction zone may then be organized into three distinct decks when the Reynolds number is high (see Fig. 1): an outer layer external to the boundary layer, consisting of inviscid disturbance flow associated with the viscous displacement effect of the underlying decks; a middle layer containing a rotational particle-isentropic nonadiabatic disturbance flow dependent on the boundary-layer profile; and a thin inner deck of nonadiabatic viscous disturbance flow within the linear portion of this profile that is interactively coupled with the local pressure field. In terms of the basic small perturbation parameter $\varepsilon \equiv Re_L^{-1/8}$, these decks have thicknesses of the order of $\varepsilon^3 L$, $\varepsilon^4 L$, and $\varepsilon^5 L$, respectively, along a streamwise interaction zone length of the order of $\varepsilon^3 L$. The triple-deck theory is used in its leading high-Reynolds-number approximation ($\varepsilon \to 0$), recast into a form suited to nonadiabatic flows by means of the reference-temperature concept combined with total enthalpy formulation of the energy equation.[3] We also adopt the pressure–deflection angle relationship given by the tangent wedge approximation, which is known to be accurate throughout the combined supersonic–hypersonic flow regimes. Assuming that $\mu \sim T^{\omega}$, the Eckert reference-temperature-based expressions for the incoming boundary-layer properties of wall shear stress, heat transfer, and atom mass diffusion are

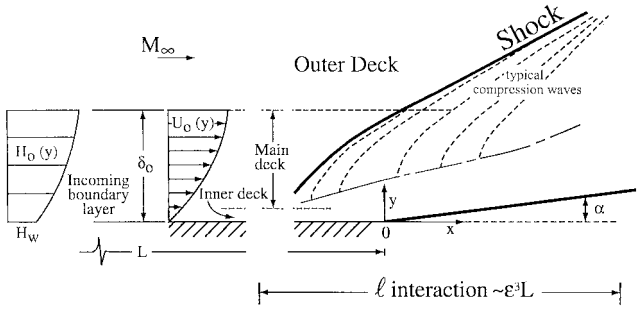

Fig. 1 Schematic of the interaction zone triple-deck structure for small $\varepsilon = Re_L^{-1/8}$.

$$\left(\frac{dU_0}{dy}\right)_w = \frac{\upsilon_{w_0}}{\mu_{w_0}} = \lambda\varepsilon^4 \left(\frac{C_{REF}^{\frac{1}{2}} T_{REF}}{T_\infty}\right)^{-1} \left(\frac{T_{REF}}{T_w}\right)^{\omega} \rho_\infty U_\infty^2 / \mu_\infty \tag{1}$$

$$-\dot{q}_{w_0} = \upsilon_{w_0}(H_{ADIAB} - C_p T_w)/ U_\infty P_R^{\frac{2}{3}} \tag{2}$$

$$\left(\frac{d\alpha_0}{dy}\right)_w = \Gamma_{c0}\,\alpha_{0_w} = \left(\frac{\upsilon_{w_0}}{U_\infty S_c^{\frac{2}{3}}}\right) \alpha_{e_0} \Gamma_{c0}(1 - \Gamma_G I_R)/(1 + \Gamma_{c0})\mu_\infty \tag{3}$$

where Γ_{c0} is the usual flat plate Damköhler number for arbitrary first-order surface catalytic recombination, and the term $\Gamma_G I_R$ (see Appendix) accounts for any nonequilibrium gas-phase reaction in the upstream boundary layer.[4]

Now introduce the following nondimensional rescaled triple-deck variables $\hat{x}, \hat{y}, \hat{u}, \hat{v}, \hat{p}, \hat{H}, \hat{\theta}, \hat{\delta}$ for streamwise and normal distance, streamwise and normal velocity, pressure perturbation, total enthalpy, deflection angle, and displacement thickness, respectively[3,5]:

$$\hat{x} \equiv (x/L)\lambda^{\frac{5}{4}}\beta^{\frac{3}{4}} / \varepsilon^3 C_{REF}^{\frac{3}{8}} (T_{REF}/T_\infty)^{\frac{3}{2}} (T_w/T_{REF})^{\omega+\frac{1}{2}} \tag{4}$$

$$\hat{y} \equiv (y/L)\lambda^{\frac{3}{4}}\beta^{\frac{1}{4}} / \varepsilon^5 C_{REF}^{\frac{5}{8}} (T_{REF}/T_\infty)^{\frac{3}{2}} (T_w/T_{REF})^{\omega+\frac{1}{2}} \tag{5}$$

$$\hat{u} \equiv (u/U_\infty)\beta^{\frac{1}{4}} / \varepsilon C_{REF}^{\frac{1}{8}} \lambda^{\frac{1}{4}} (T_w/T_\infty)^{\omega+\frac{1}{2}} \tag{6}$$

$$\hat{v} \equiv (v/U_\infty) / \varepsilon^3 \beta^{\frac{1}{4}} C_{REF}^{\frac{3}{8}} \lambda^{\frac{3}{4}} (T_w/T_\infty)^{\frac{1}{2}} \tag{7}$$

$$\hat{p} \equiv \left[\frac{(p - p_\infty)}{\rho_\infty U_\infty^2}\right] \beta^{\frac{1}{2}} / \varepsilon^2 C_{REF}^{\frac{1}{4}} \lambda^{\frac{1}{2}} \tag{8}$$

$$\hat{H} \equiv \beta^{\frac{1}{4}}(H - C_p T_w) / P_r^{\frac{1}{3}} (H_{ADIAB} - C_p T_w) \varepsilon C_{REF}^{\frac{1}{8}} \lambda^{\frac{1}{4}} (T_w/T_\infty)^{\frac{1}{2}} \tag{9}$$

$$\hat{\theta} \equiv \theta / \varepsilon^2 \lambda^{\frac{1}{2}} \beta^{\frac{1}{2}} C_{REF}^{\frac{1}{4}} \tag{10}$$

$$\hat{\delta} \equiv (\delta^*/L)\lambda^{\frac{3}{4}}\beta^{\frac{1}{4}} / \varepsilon^5 C_{REF}^{\frac{3}{8}} (T_{REF}/T_\infty)^{\frac{3}{2}} (T_w/T_{REF})^{\omega+\frac{1}{2}} \tag{11}$$

Further add the comparable partial total enthalpy (excluding dissociation energy contribution) and atom mass fraction variables:

$$H = C_p T + U^2/2 \tag{12}$$

$$\hat{\alpha} = \beta^{\frac{1}{4}} \alpha / S_c^{\frac{1}{3}} \alpha_{e_0} \Gamma_{c0}(1 - \Gamma_G I_R)(1 + \Gamma_{c0})^{-1} \varepsilon C_{REF}^{\frac{1}{8}} \lambda^{\frac{1}{4}} (T_w/T_\infty)^{\frac{1}{2}} \tag{13}$$

Then, in the leading asymptotic approximation $\varepsilon \to 0$, it is found after detailed analysis that the mass, momentum, energy, and species conservation equations for the combined three decks take the following form:

$$\frac{\partial \hat{u}}{\partial \hat{x}} + \frac{\partial \hat{v}}{\partial \hat{y}} = 0 \tag{14}$$

$$\hat{u}\frac{\partial \hat{u}}{\partial \hat{x}} + \hat{v}\frac{\partial \hat{v}}{\partial \hat{y}} + \frac{d\hat{p}}{d\hat{x}} = \frac{\partial^2 \hat{u}}{\partial \hat{y}^2} \tag{15}$$

$$\hat{u}\frac{\partial \hat{H}}{\partial \hat{x}} + \hat{v}\frac{\partial \hat{H}}{\partial \hat{y}} = P_R^{-1}\frac{\partial^2 \hat{H}}{\partial \hat{y}^2}$$

$$+ \varepsilon^2 \hat{h}_D\, \hat{\Gamma}_G\left[g_{\alpha_0}(\hat{\alpha} - \hat{y}) + \lambda_T g_{T_0}(\hat{T} - \hat{y})\right] \tag{16}$$

$$\hat{u}\frac{\partial \hat{\alpha}}{\partial \hat{x}} + \hat{v}\frac{\partial \hat{\alpha}}{\partial \hat{y}} = S_c^{-1}\frac{\partial^2 \hat{\alpha}}{\partial \hat{y}^2} - \varepsilon^2 \hat{\Gamma}_G\left[g_{\alpha_0}(\hat{\alpha} - \hat{y}) + \lambda_T g_{T_0}(\hat{T} - \hat{y}^2)\right] \tag{17}$$

$$\hat{p} = \hat{s}_e\left[\sqrt{1 + (K_H \hat{s}_e)^2} + K_H \hat{s}_e\right] \qquad \text{with} \qquad \hat{s}_e \equiv \frac{\mathrm{d}}{\mathrm{d}\hat{x}}\left(\hat{y}_B + \hat{\delta}^*\right) \tag{18}$$

where $\hat{T}$ is the rescaled temperature variable and negligibly small transport terms proportional to $1 - P_R$ and $(1 - P_R/S_c)$ have been neglected on the right-hand side of energy equation (16). Several terms pertaining to ultracold wall effects have also been omitted in Eqs. (15) and (18) owing to their insignificance for practical flow conditions.[3] The foregoing equations are to be solved subject to the inner–outer matching conditions that

$$\hat{u}(\hat{x}, \hat{y} \to \infty) = \hat{y} - \hat{y}_B - \hat{\delta}^* \tag{19}$$

$$\hat{H}(\hat{x}, \hat{y} \to \infty) = \hat{y} - \hat{y}_B - \hat{\delta}^*$$

$$+ \frac{\varepsilon^3 \hat{h}_D \hat{\Gamma}_G}{(\varepsilon \hat{y})}\left(g_{\alpha_0} + \lambda_T g_{T_0}\right)\int_{-\infty}^{\hat{x}} \left(\hat{y}_B + \hat{\delta}^*\right)\mathrm{d}\hat{x} \tag{20}$$

$$\hat{\alpha}(\hat{x}, \hat{y} \to \infty) = \hat{y} - \hat{y}_B - \hat{\delta}^*$$

$$- \frac{\varepsilon^3 \hat{\Gamma}_G}{(\varepsilon \hat{y})}\left(g_{\alpha_0} + \lambda_T g_{T_0}\right)\int_{-\infty}^{x^3} \left(\hat{y}_B + \hat{\delta}^*\right)\mathrm{d}\hat{x} \tag{21}$$

while on the impermeable wall ($\hat{y}_B = 0$ for $\hat{x} < 0$, $\hat{y}_B = \hat{\theta}_B \hat{x}$ for $\hat{x} \geq 0$) of arbitrary temperature and first-order catalycity we have the boundary conditions $\hat{u} = \hat{v} = \hat{H} = 0$ plus

$$\frac{\partial \hat{\alpha}}{\partial \hat{y}}(\hat{x}, 0) = \hat{\Gamma}_{i_w}\alpha(\hat{x}, 0) \tag{22}$$

where $\hat{\Gamma}_{i_w}$ is a new interactive catalytic Damköhler number proportional to Γ_{c0} that contains an additional y-scaling factor associated with the inner deck.

An important conclusion regarding the influence of gas-phase reaction can now be drawn by direct inspection of the foregoing equations. Thus Eqs. (16) and (17) show that, unless this recombination–dissociation reaction is very close to equilibrium ($\hat{\Gamma}_G \gg 1$), its relative effect even on the slow inner deck flow near the wall is of the order of ε^2 compared with the effects of convection and diffusion and thus may be neglected for the purposes of a first-order triple-deck analysis. In fact, examination of the outer matching conditions with the middle deck, where $\varepsilon\hat{y}$ is of the order of unity [Eqs. (20) and (21)], shows that the relative gas-phase reaction effect in the upper part of the triple-deck structure is of the order of ε^3 and hence even smaller. Physically, the foregoing imply that, owing to the very short streamwise scale of a typical shock interaction zone, we may in effect regard any finite-rate gas-phase reaction as chemically frozen across the entire triple-deck structure along the zone. Note, however, that the influence at the chemical history upstream of the interaction, however arbitrary, can be readily accommodated in the theory by means of Eqs. (3), (13), and (22).

III. Solution Results and Discussion

The foregoing universal split-boundary-value problems for Eqs. (14–16) and (18), which are uncoupled from the atom species problem, have in fact been widely investigated both analytically and numerically[6] over the range of wedge angles $0 \leq \hat{\theta}_B \leq 1.57$ pertaining to unseparated flow; a typical example of the resulting interactive pressure distribution is shown in Fig. 2a. The attendant atom species

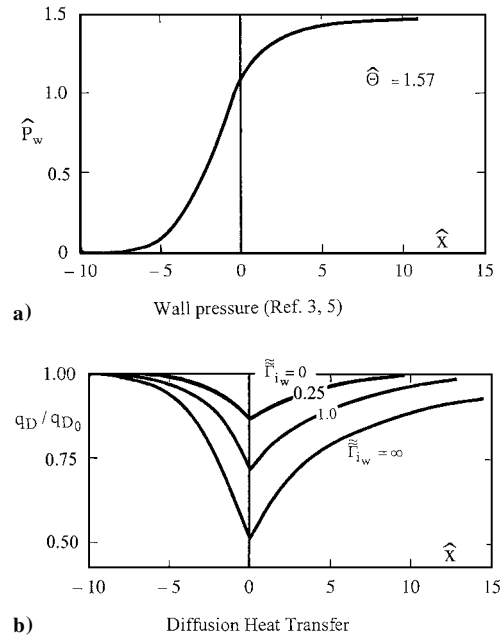

Fig. 2 Typical interaction effect on local diffusional heat transfer vs $\tilde{\tilde{\Gamma}}_{i_w}$ for $\hat{\theta} = 1.57$.

problem defined by Eqs. (17), (20), and (21) is, however, new and has not been studied. Although a numerical solution of it could of course be done, it was chosen instead for the present purposes to provide an approximate analytical solution to bring out the essential effects of finite surface catalycity on the local interaction zone heating.

To do this, we consider the special case of $P_R = S_c = 1$ (this has long been known to capture the main essentials of hypersonic-reacting viscous-flow heating[6]). Differentiate Eq. (15) with respect to $\hat{y}$ so as to eliminate $\hat{p}$ and then use continuity equation (14) to obtain the interactive vorticity equation

$$\left\{\hat{u}\frac{\partial}{\partial \hat{x}} + \hat{v}\frac{\partial}{\partial \hat{y}} - \frac{\partial^2}{\partial \hat{y}^2}\right\}\left(\frac{\partial \hat{u}}{\partial \hat{y}}\right) = 0 \tag{23}$$

subject to the outer condition that $\partial\hat{u}/\partial\hat{y}(\hat{x}, \hat{y} \to \infty) = 1$. Then, with $P_R = S_c = 1$, a comparison of Eqs. (16), (17), and (22) shows that $\hat{\alpha}$ obeys a kind of interactive Crocco relationship in which it is a linear combination of $\partial\hat{u}/\partial\hat{y}$ and $\hat{H}$ of the form $\hat{\alpha} = C_1 + C_2(\partial\hat{u}/\partial\hat{y}) + C_3\hat{H}$, where C_1, C_2, and C_3 are arbitrary constants. Then the outer matching conditions require that $C_1 = 1$ and $C_3 = -C_2$, whereas the wall compatibility condition from Eq. (15) requires that $\partial^2\hat{u}/\partial\hat{y}^2(x, 0) = \mathrm{d}\hat{p}/\mathrm{d}\hat{x}$ plus the wall boundary condition $\hat{H}(\hat{x}, 0) = 0$ yield in connection with Eq. (21) the value

$$C_2 = -\left(\frac{\partial \hat{H}}{\partial \hat{y}}\right)_w \Bigg/ \left\{\left(\frac{\mathrm{d}\hat{p}}{\mathrm{d}x}\right)_w + \hat{\Gamma}_{i_w}\left[1 - \left(\frac{\partial \hat{u}}{\partial \hat{y}}\right)_w\right]\right\}$$

where the various wall values here are all known from the existing solutions mentioned earlier. We especially note that these values each vanish at exactly the same (exponential) streamwise rate in the upstream influence region, whereas they approximately do so algebraically downstream of the wedge corner; consequently, C_2 can be taken as essentially a known constant along the interaction. Differentiating the $\hat{\alpha}$ solution mentioned earlier with respect to $\hat{y}$ and substituting these constants, we find that the final result for the atom diffusion flux into the wall (to which the local diffusional heating is proportional) is

$$\left(\frac{\partial \hat{\alpha}}{\partial y}\right)_w = \left(\frac{\tilde{\tilde{\Gamma}}_{i_w}}{1 + \tilde{\tilde{\Gamma}}_{i_w}}\right)\left(\frac{\partial \hat{H}}{\partial y}\right)_w \tag{24}$$

where $\tilde{\tilde{\Gamma}}_{i_w} \equiv \hat{\Gamma}_{i_w}[1 - (\partial\hat{u}/\partial\hat{y})_w]/(\mathrm{d}\hat{p}/\partial\hat{x})$ is yet another effective interactive catalytic Damköhler number that weakly varies along the interaction. Clearly, Eq. (24) enables the direct use of already known

nonreacting flow values of the wall enthalpy gradient[4] (which is defined so as to equal unity far upstream) to assess the influence of arbitrary degrees of finite surface catalycity ranging from fully catalytic ($\tilde{\tilde{\Gamma}}_{i_w} \to \infty$) to completely noncatalytic($\tilde{\tilde{\Gamma}}_{i_w} \to 0$). Equation (24) also implies that the diffusive heat flux, like the conductive heating, is proportional to the local interactive wall enthalpy gradient and hence is reduced by the local interactive pressure rise.[4] Theoretical results for the typical shock-impingement effect on the local relative diffusional heating are shown in Fig. 2b as functions of typical values for $\tilde{\tilde{\Gamma}}_{i_w}$. It is seen that the maximum effect, which reduces heating to a minimum at the shock foot, occurs for a fully catalytic wall ($\tilde{\tilde{\Gamma}}_{i_w} = \infty$), whereas there is no response at all on a completely noncatalytic wall ($\tilde{\tilde{\Gamma}}_{i_w} = 0$). Intermediate degrees of catalytic effect pertain to the range of values $0.01 \le \tilde{\tilde{\Gamma}}_{i_w} \le 10.0$. When assessing effects on the absolute local diffusive flux, one must of course take into account that the upstream value is also influenced by the surface catalycity.

IV. Conclusion

Although there appear to be no data on nonequilibrium heat transfer in dissociated-flow interaction zones that could be used to verify the foregoing theory, the prediction of Eq. (24) that the local diffusive heating be proportional to the corresponding conduction heat transfer has been qualitatively checked against the local heat transfer distributions measured by Needham[7] in a Mach 9.7 interacting corner flow.[8]

Appendix: Details of the Specie Conservation Equation

The atom specie conservation equation governing the nonequilibrium-dissociated flow in a laminar boundary layer is[9]

$$\rho\left(u\frac{\partial\alpha}{\partial x}+v\frac{\partial\alpha}{\partial y}\right)-\frac{\partial}{\partial y}\left(\frac{\mu}{S_c}\frac{\partial\alpha}{\mathrm{d}y}\right)=-2\rho\kappa_R' T^{\omega-2}\left(\frac{p_e}{R_u}\right)^2 g(\alpha,T) \tag{A1}$$

where κ_R' is the recombination rate constant and $g(\alpha, T)$ is the net reaction rate function:

$$g(\alpha,T)=\frac{\alpha^2}{1+\alpha}-\frac{\alpha_e^2(1-\alpha)}{\left(1-\alpha_e^2\right)}\exp\left[-\frac{h_D}{R_m T}\left(1-\frac{T}{T_e}\right)\right] \tag{A2}$$

When the lengths and the velocities in Eq. (A1) are normalized by L and U_∞, respectively, the resulting nondimensional reaction term on the right-hand side takes the form $\rho\Gamma_G(T/T_e)^{\omega-2}g(\alpha,T)$, where

$$\Gamma_G \equiv 2\kappa_R' T_e^{\omega-2} L(p_e/R_u)^2/U_\infty \tag{A3}$$

is the characteristic convection time to reaction time ratio or homogeneous Damköhler number. The limit $\Gamma_G \to 0$ thus pertains to a chemically frozen flow, whereas the opposite limit $\Gamma_G \to \infty$ with $g \to 0$ pertains to locally chemical equilibrium flow. We note that, for finite nonequilibrium reactions, the variation of g due to small perturbations in α and T about some reference state α_0, T_0 can be expressed by the Taylor series expansion

$$g = g_0(\alpha_0,T_0)+g_{\alpha_0}\cdot(\alpha-\alpha_0)+g_{T_0}\cdot(T-T_0)+\cdots \tag{A4}$$

where $g_{\alpha_0} \equiv (\partial g/\partial\alpha)_0$ and $g_{T_0} \equiv (\partial g/\partial T)_0$. This was in fact used in obtaining Eqs. (16), (17), (20), and (21) of the text, in which the modified interactive Damköhler number (proportional to Γ_G), defined by

$$\hat{\Gamma}_G \equiv \frac{C_{\mathrm{REF}}^{\frac{1}{4}}(T_{\mathrm{REF}}/T_\infty)^{1-\omega}}{\beta^{\frac{1}{2}}\lambda^{\frac{3}{2}}}\cdot\Gamma_G \tag{A5}$$

was introduced. If the reference state is the incoming boundary layer upstream of the shock boundary-layer interaction zone, which is usually locally similar to a good approximation, it can be shown[5] that the solution of Eq. (A1) for the properties at an arbitrarily catalytic surface gives the result cited in Eq. (3), where

$$\Gamma_{c0} = S_c^{\frac{2}{3}}(\kappa_w/U_\infty)\sqrt{2Re_L/C_{\mathrm{REF}}}/\lambda \tag{A6}$$

is the characteristic diffusion time to surface recombination time ratio or heterogeneous Damköhler number, and I_R in Eq. (3) is a gas-phase reaction rate integral of the function g across the boundary layer given in Ref. 4.

References

[1] Grumet, A., Anderson, J. D., and Lewis, M. J., "A Numerical Study of the Effects of Wall Catalysis on Shock Wave/Boundary Layer Interaction," *Journal of Thermophysics and Heat Transfer*, Vol. 8, No. 1, 1994, pp. 40–47.

[2] Inger, G. R., "Hypersonic Oblique Shock Interaction with a Laminar Boundary Layer," *International Journal of Turbo and Jet Engines*, Vol. 7, No. 6, 1990, pp. 309–330.

[3] Inger, G. R., "Theory of Local Heat Transfer in Shock/Laminar Boundary-Layer Interactions," *Journal of Thermophysics and Heat Transfer*, Vol. 12, No. 3, 1998, pp. 336–342.

[4] Inger, G. R., "Nonequilibrium Boundary Layer Effects on the Aerodynamic Heating of Hypersonic Waverider Vehicles," *Journal of Thermophysics and Heat Transfer*, Vol. 9, No. 4, 1995, pp. 595–604.

[5] Rizzetta, D. P., "Asymptotic Solutions of the Energy Equation for Viscous Supersonic Flow Past Corners," *Physics of Fluids*, Vol. 22, No. 1, 1979, pp. 218–223.

[6] Hayes, W. D., and Probstein, R. F., *Hypersonic Flow Theory*, Academic, New York, 1959, pp. 293–312.

[7] Needham, D., "A Heat Transfer Criterion for the Detection of Incipient Separation in Hypersonic Flow," *AIAA Journal*, Vol. 4, No. 5, 1966, pp. 790–799.

[8] Inger, G. R., "Shock/Viscous Interaction Effects on Nonequilibrium-Dissociated Heating Along Arbitrarily-Catalytic Surfaces," AIAA Paper 98-2814, June 1998.

[9] Fay, J. A., and Riddell, F. R., "Theory of Stagnation Point Heat Transfer in Dissociated Air," *Journal of the Aeronautical Sciences*, Vol. 25, No. 2, 1958, pp. 73–85.

Gas Permeability of Lightweight Ceramic Ablators

Jochen Marschall*
NASA Ames Research Center,
Moffett Field, California 94035-1000
and
Michael E. Cox†
San Jose State University,
San Jose, California 95192-0087

Nomenclature

b	= permeability slip parameter, Pa
D	= sample diameter, m
K	= effective permeability, m^2
K_0	= continuum flow permeability, m^2
L	= length, m
M	= molar mass, kg-mol^{-1}
$\dot{m}$	= mass flow rate, kg-s^{-1}
P	= pressure, Pa
P_{av}	= average pressure across sample, Pa
R	= universal gas constant, J-mol^{-1}-K^{-1}
T	= temperature, K
ΔP	= pressure difference across sample, Pa
μ	= viscosity, Pa-s

Received 6 October 1998; revision received 17 December 1998; accepted for publication 17 December 1998.

*Senior Research Scientist, Thermosciences Institute, ELORET Corporation, M/S 234-1; jmarschall@mail.arc.nasa.gov.

†Student, Department of Chemical Engineering.